Quantum Structure in the Dielectric Function of Metals and Anomalous Propagation Modes*

A. J. GLICK†
Department of Physics and Astronomy, University of Maryland, College Park, Maryland
AND
EARL CALLEN‡
U. S. Naval Ordnance Laboratory, White Oak, Silver Spring, Maryland
(Received 25 October 1967; revised manuscript received 26 January 1968)

Semiclassically, the dielectric constant of a free-electron gas in a magnetic field is highly absorptive within the cone $\omega=\omega_c\pm v_F q$. But quantum mechanically, within this region there are many large "windows" in which the absorptive component $\epsilon_2^-(\omega,q)=0$. In the first part of this paper we describe these large windows in detail. We then consider propagation within them. We show that in a nonmagnetic material there are other solutions of the dispersion relation in addition to a heliconlike mode. We next consider a ferromagnetic metal, and predict that in nickel a propagating magnon-helicon mode may exist up to microwave frequencies for wave numbers up to $q\simeq 10^6$ cm^{-1}, which is 10^3 times the q of the Kjeldaas edge. The usual microwave transmisson or reflection experiments are not suited to the observation of these effects, or the related phenomenon of giant quantum oscillations in helicon attenuation which has been previously predicted. To be successful, an experiment must be able to determine both the frequency and the wave number of the absorption process. Perhaps inelastic photon (Raman) scattering could be used for this purpose.

I. INTRODUCTION

HELICON oscillations[1–4] have been employed to study many physical properties of metals including the Hall coefficient and magnetoresistance.[5] In the semiclassical theory of the complex dielectric function tensor $\epsilon(\omega,q)$ of a free-electron gas in a magnetic field[6–8] upon which the helicon dispersion relation depends, there is an imaginary part which comes from Doppler-shifted cyclotron-resonance excitation.[9] These excitations have a sudden onset at what corresponds to the Kjeldaas edge, which is perhaps best-known in connection with magnetoacoustic absorption.[10] Stern[11] pointed out that the abrupt increase in helicon attenuation at this edge can be employed to map out the Fermi surface.

The physical origin of this absorption is easily understood. Suppose that a helicon of frequency ω and wave number q propagates parallel to a magnetic field H applied to the metal. An electron on the Fermi surface whose velocity component is $\pm v$ along the direction of H and q then experiences an oscillatory electromagnetic field of Doppler-shifted frequency

$$\omega'=\omega\mp vq. \tag{1.1}$$

If ω' coincides with the cyclotron frequency ω_c of the electron, energy will be absorbed from the helicon. Thus the semiclassical theory predicts absorption for frequencies everywhere within the cone

$$\omega=\omega_c\pm v_F q. \tag{1.2}$$

Stern and Callen[12] discussed this absorption in another context. They considered a magnetic metal with ferromagnetically aligned spins embedded in the conduction electron gas. The permeability of the localized spins was obtained from the Landau-Lifshitz equation, and the dielectric constant of the free-electron gas was taken from the semiclassical theory.[6,8] At room temperature there is a strong interaction between the electromagnetic field and spin-wave excitations only near $q=0$, where the spectra are degenerate.[13–17] But under the low-temperature, high-purity conditions $\omega_c\tau>1$ necessary for helicon propagation, there is a large interaction between electromagnetic and magnon modes for a very wide range of momenta. This interaction is due to the time-varying magnetic fields of the precessing spins which induce large displacement currents in the high-conductivity gas. The currents in turn set up magnetic fields which act back on the spin system. Because the dielectric

* A preliminary and brief summary of this work has appeared in Phys. Letters **20**, 574 (1966).
† Supported in part by U. S. Air Force Office of Scientific Research under Grant No. AF-AFOSR-735-65.
‡ Department of Physics, American University, Washington, D. C.
[1] R. Bowers, C. Legendy, and F. Rose, Phys. Rev. Letters **7**, 339 (1961).
[2] F. Rose, M. Taylor, and R. Bowers, Phys. Rev. **127**, 1122 (1962).
[3] R. G. Chambers and B. K. Jones, Proc. Roy. Soc. (London) **A270**, 417 (1962).
[4] P. Cotti, P. Wyder, and A. Quattropani, Phys. Letters **1**, 50 (1962).
[5] M. T. Taylor, J. R. Merrill, and R. Bowers, Phys. Rev. **129**, 2525 (1963).
[6] R. G. Chambers, Phil. Mag. **1**, 459 (1956).
[7] M. H. Cohen, M. J. Harrison, and W. A. Harrison, Phys. Rev. **117**, 937 (1960).
[8] P. B. Miller and R. R. Haering, Phys. Rev. **128**, 126 (1962).
[9] J. Kirsch and P. B. Miller, Phys. Rev. Letters **9**, 421 (1962).
[10] T. Kjeldaas, Jr., Phys. Rev. **113**, 1473 (1959).
[11] Edward A. Stern, Phys. Rev. Letters **10**, 91 (1963).
[12] Edward A. Stern and Earl Callen, Phys. Rev. **131**, 512 (1963).
[13] W. S. Ament and G. T. Rado, Phys. Rev. **97**, 1558 (1955).
[14] C. Kittel, Phys. Rev. **110**, 840 (1958).
[15] P. Pincus, Phys. Rev. **118**, 658 (1960).
[16] B. A. Auld, J. Appl. Phys. **31**, 1642 (1960).
[17] R. F. Soohoo, Phys. Rev. **120**, 1978 (1960).

function employed by Stern and Callen contains an imaginary part, however, coupled modes with an appreciable electromagnetic component are predicted to be strongly absorbed everywhere within the semiclassical cone of Eq. (1.2).

In a quantum-mechanical treatment of the dielectric function tensor the viewpoint and conclusions are somewhat different. Quinn and Rodriguez[18] and Zyryanov and Kalashnikov[19] have derived the transverse circularly polarized component of the conductivity tensor of the free-electron gas which is appropriate to this case. Because of the external magnetic field (or the magnetization), the single-electron states break into quantized Landau levels. The absorption processes which can occur are strongly determined by Pauli exclusion restrictions, since an electron absorbing a helicon of energy $\hbar\omega$ must initially occupy a state within the Fermi sea, and must transfer to an empty state outside. The magnetic field is taken in the z direction, and we consider helicons propagating along z with momentum $\hbar q$. In the absorption process, conservation of energy and momentum require that the final- and initial-electron states differ in frequency by ω, and in z component of wave number by q. The matrix elements of the perturbative electromagnetic field between the Hermite polynomials of the electronic wave functions give rise to the additional selection rule $\Delta n=\pm 1$ (the positive sign for left circular polarization), where the index n labels the Landau levels. These conservation and selection rules, and most particularly Pauli exclusion, cause the quantum-mechanical dielectric tensor to have a complex structure. The effect of this structure on helicon attenuation was considered by Quinn[20] and by Miller.[21] Similar structure effects have been investigated in connection with magnetoacoustic absorption; Gurevich, Skobov, and Firsov[22] showed how $\Delta n=0$ transitions cause "giant quantum oscillations" in the attenuation of longitudinal sound waves. In the case of transverse waves, where the $\Delta n=\pm 1$ transitions apply, there are giant oscillations in sound attenuation, as described by Langenberg, Quinn, and Rodriguez[23] and by Gantsevich and Gurevich.[24] These latter arise from the same filamentary fine structure along the Kjeldaas edge in the component $\epsilon_2^-(\omega,q)$ which causes the oscillations in helicon attenuation.[20,21]

Section II of the present paper contains a detailed analytic and graphical description of $\epsilon_2^-(\omega,q)$. We shall show that in addition to the filamentary structure already discussed[20,21,23,24] there are large "windows," regions in which $\epsilon_2^-(\omega,q)=0$, within the cone of Eq. (1.2). These windows exist far beyond the Kjeldaas edge, and extend over a frequency range which is 10^4 times wider than the filamentary fine structure near the edge. We limit our attention to transverse waves, hence to $\Delta n=\pm 1$ transitions, and to the transverse components of the dielectric tensor. We are neglecting electron spin in this description. However, it is easily shown that with a spherical Fermi surface and an electronic g factor of 2 the absorption due to spin-flip processes will give rise to an identical window structure and will not alter any of our conclusions. More generally it can give rise to additional spin-flip filaments with similar qualitative features.

Windows in $\epsilon_2^-(\omega,q)$ can be observed experimentally if well-defined propagating modes exist with dispersion curves $\omega(q)$ passing through the window region. We shall describe such propagating modes in two systems. In Sec. III we consider a pure nonmagnetic metal such as sodium, in a large magnetic field. In Sec. IV we consider coupled helicon-magnon modes in a ferromagnetic metal such as nickel. In both cases, of course, Maxwell's equations lead to the dispersion relation

$$\omega^2=c^2q^2/\mu\epsilon, \tag{1.3}$$

with $\mu(\omega,q)$ and $\epsilon(\omega,q)$ to be taken from appropriate model calculations. In the nonmagnetic metal we ignore the small permeability of the free-electron gas, set $\mu(\omega,q)=1$, and employ the quantized complex, nonlocal dielectric function. In the ferromagnetic metal the distinction between $\mu(\omega,q)$ and $\epsilon(\omega,q)$ is not so clear cut, but to a good approximation we can ignore cross terms, calculating the permeability of the spin system from the Landau-Lifshitz equation, and the dielectric constant of the gas from the free-electron model.

In both cases we find interesting solutions to the dispersion relation (1.3). The existence of these solutions can be inferred most easily from the structure of $\epsilon_2^-(\omega,q)$ and the Kramers-Kronig relation which relates $\epsilon_2^-(\omega,q)$ and $\epsilon_1^-(\omega,q)$. A logarithmic singularity occurs in $\epsilon_1^-(\omega,q)$ at each discontinuity in $\epsilon_2^-(\omega,q)$, and these logarithmic spikes in $\epsilon_1^-(\omega,q)$ enforce solutions of Maxwell's equations which lie between filaments in $\epsilon_2^-(\omega,q)$. These solutions will be illustrated for nonmagnetic metals in Sec. III. Their presence modifies our picture of giant quantum oscillations in helicon attenuation.[20,21] The analysis indicates that observation of these oscillations will be impossible unless both ω and q are experimentally fixed. With the highly coherent photon source available from a laser, it may be possible to study effects of this structure on photon scattering (Raman effect). However near the Kjeldaas edge the filaments are so narrow that detection will be difficult.

In the ferromagnetic metal the large permeability

[18] J. J. Quinn and S. Rodriguez, Phys. Rev. **128**, 2487 (1962).
[19] P. S. Zyryanov and V. P. Kalashnikov, Zh. Eksperim. i Teor. Fiz. **41**, 1119 (1961) [English transl.: Soviet Phys.—JETP **14**, 799 (1962)].
[20] J. J. Quinn, Phys. Letters **7**, 235 (1963).
[21] P. B. Miller, Phys. Rev. Letters **11**, 537 (1963).
[22] V. L. Gurevich, V. G. Skobov, and Yu A. Firsov, Zh. Eksperim. i Teor. Fiz. **40**, 786 (1961) [English transl.: Soviet Phys.—JETP **13**, 552 (1961)].
[23] D. N. Langenberg, J. J. Quinn, and S. Rodriguez, Phys. Rev. Letters **12**, 104 (1964).
[24] S. V. Gantsevich and V. L. Gurevich, Zh. Eksperim. i Teor. Fiz. **45**, 587 (1963) [English transl.: Soviet Phys.—JETP **18**, 403 (1964)].

has a decisive effect. Within very large windows at wave numbers up to $q\simeq 10^6$ cm^{-1}, we find a propagating mode, whose frequency ultimately coincides with that of the uncoupled spin wave. This mode is the continuation, within the semiclassical absorption cone, of the lower branch of the spectrum discussed by Stern and Callen.[12] But while those authors considered the mode to terminate at the Kjeldaas edge, the present quantum-mechanical calculation predicts propagation far beyond the edge, where there is a good possibility of experimental detection.

II. DIELECTRIC CONSTANT

The complex dielectric function tensor of a quantum plasma in a uniform magnetic field has been calculated by Zyryanov and Kalashnikov[19] and by Quinn and Rodriguez[18] from the equation of motion of the density matrix in the presence of a small electromagnetic perturbation. We restrict ourselves to the special case of propagation along the magnetic field direction. Letting

$$\epsilon^{\pm}(\omega,q)=\epsilon_1{}^{\pm}+i\epsilon_2{}^{\pm} \tag{2.1}$$

be the components of the complex dielectric function tensor for circularly polarized propagation, one finds[18] (in terms of symbols defined below)

$$\epsilon_1{}^{-}=1-\frac{\omega_p{}^2}{\omega^2}\Bigg\{1+\tfrac{3}{2}u_c\beta \times\sum_{n=0}^{n_F}\ln\Bigg|\Bigg(\frac{[1-\beta(2n+1)]^{1/2}+u_c-u-z}{[1-\beta(2n+1)]^{1/2}-u_c+u+z}\Bigg)^{n} \times\Bigg(\frac{[1-\beta(2n+1)]^{1/2}-u_c+u-z}{[1-\beta(2n+1)]^{1/2}+u_c-u+z}\Bigg)^{n+1}\Bigg|\Bigg\}, \tag{2.2}$$

$$\epsilon_2{}^{-}=\frac{(m\omega_c)^2}{(4\pi N/V)\hbar^2 q}\frac{\omega_p{}^2}{\omega^2}[(n_0+1)(n_0+2) -(n_1+1)(n_1+2)]. \tag{2.3}$$

In (2.3), n_0 and n_1 are the largest integers less than certain values:

$$n_0=\mathrm{Int}\Bigg[\frac{1-z^2-u_c{}^2(1-\omega/\omega_c)^2}{2\beta}-1+\frac{\omega}{2\omega_c}\Bigg],$$
$$n_1=\mathrm{Int}\Bigg[\frac{1-z^2-u_c{}^2(1-\omega/\omega_c)^2}{2\beta}-1-\frac{\omega}{2\omega_c}\Bigg]. \tag{2.4}$$

The components $\epsilon^{-}(\omega,q)$ given in (2.2) and (2.3) are appropriate for metals in which electrons move in electronlike orbits; for metals with holelike trajectories the conjugate matrix elements describe the electron-electromagnetic wave coupling. In these expressions ω_p is the plasma frequency, ω_c is the cyclotron frequency, v_F is the Fermi velocity, k_F is the Fermi wave number, and β is a dimensionless ratio:

$$\omega_p{}^2=4\pi Ne^2/mV,$$
$$\omega_c=eB/mc,$$
$$k_F=mv_F/\hbar, \tag{2.5}$$
$$\beta=\omega_c/k_Fv_F.$$

Here N/V is the number of electrons per unit volume. For definitude we assume representative values $\omega_p=1.8\times10^{16}$ sec^{-1}, $\omega_c=3.5\times10^{11}$ sec^{-1}, corresponding to $B=2\times10^4$ G, $v_F=10^8$ cm/sec, $k_F=8.6\times10^7$ cm^{-1}. Thus $\beta=4.1\times10^{-5}$; the ratio of the zero point cyclotron energy to the Fermi energy is a very small parameter. In Eqs. (2.2)–(2.4) it has been convenient to employ the dimensionless quantities

$$u=\omega/qv_F,$$
$$u_c=\omega_c/(qv_F), \tag{2.6}$$
$$z=q/(2k_F).$$

The summation index n, an integer labeling the Landau levels, runs from zero to n_F, where n_F is the largest integer such that

$$n_F\leq|\tfrac{1}{2}(1/\beta-1)|. \tag{2.7}$$

For our assumed value of β, the quantum number of the highest Landau level within the Fermi sphere is $n_F\simeq10^4$.

Although Eqs. (2.2) and (2.3) are complete, additional insight into the structure of the dielectric constant can be gained through simple considerations. To discover propagation we must first find regions in which $\epsilon_2{}^{-}(\omega,q)$ vanishes or is very small. These regions will occur for those ω's and q's for which single-particle excitations cannot occur. An electron on the nth Landau level with initial z component of momentum $\hbar k_i$ has energy

$$E_n=\frac{\hbar^2k_i{}^2}{2m}+(n+\tfrac{1}{2})\hbar\omega_c. \tag{2.8}$$

In absorption of helicon energy $\hbar\omega$ and momentum $\hbar q$, the electron will be excited to the $(n+1)$st level, and its z component of momentum will be increased by $\hbar q$. Then by energy conservation

$$\omega=\omega_c+(\hbar/m)(k_iq+\tfrac{1}{2}q^2). \tag{2.9}$$

However k_i must lie within the Fermi surface so that

$$|k_i(n)|\leq[k_F{}^2-(n+\tfrac{1}{2})k_c{}^2]^{1/2}, \tag{2.10}$$

where we have defined a convenient "cyclotron wave number"

$$k_c\equiv(2m\omega_c/\hbar)^{1/2}. \tag{2.11}$$

In addition the Pauli principle restricts the allowed values of q to those which result in final states outside the Fermi sea for each k_i. Since q is non-negative, Eq. (2.9) shows that transitions initiating in the right Fermi hemisphere ($k_i>0$) are associated with frequen-

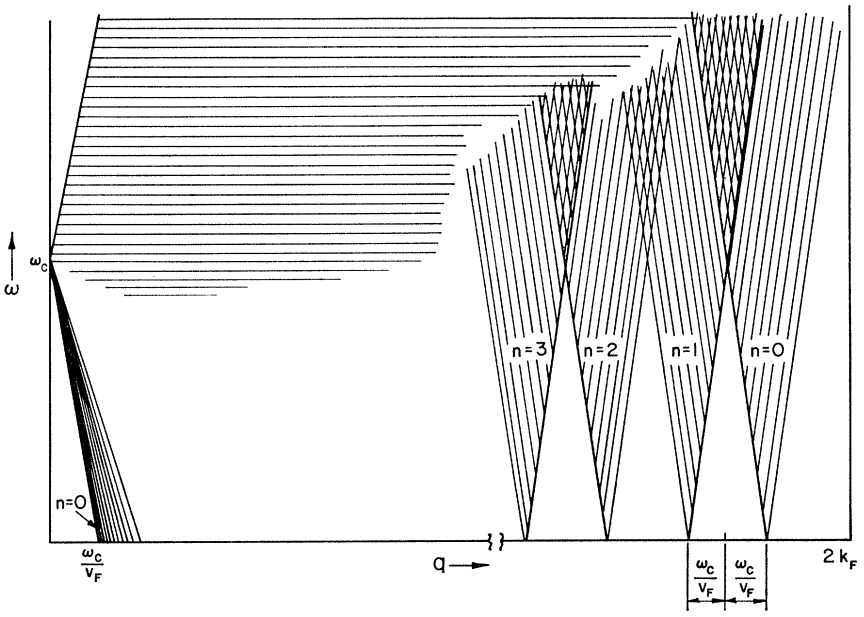

FIG. 1. Regions of the ω-q plane showing where the imaginary part of the dielectric constant is nonzero due to energy absorptions by electrons excited from the inner Landau levels.

cies $\omega \geq \omega_c$. The interesting quantum effects which we will describe are all associated with frequencies lower than ω_c, and thus with $k_i<0$. We first consider the k_i which correspond to states which lie on the Fermi surface:

$$k_i=-k_F(n)\equiv-[k_F^2-(n+\tfrac{1}{2})k_c^2]^{1/2}. \quad (2.12)$$

Equation (2.9) describes a family of parabolas parameterized by these k_i. Energy absorption can occur everywhere along the parabolas provided either

$$q\leq[k_F^2-(n+\tfrac{1}{2})k_c^2]^{1/2}-[k_F^2-(n+\tfrac{3}{2})k_c^2]^{1/2} \quad (2.13)$$

or

$$q\geq[k_F^2-(n+\tfrac{1}{2})k_c^2]^{1/2}+[k_F^2-(n+\tfrac{3}{2})k_c^2]^{1/2}. \quad (2.14)$$

The limiting equalities correspond to transitions from the Fermi surface to states on the Fermi surface and hence are associated with $\omega=0$. For q's away from these limits the transitions correspond to energy absorptions, and hence to the positive frequency portions of the parabolas. For values of k_i which are not on the Fermi surface, the electron must be raised from below to above the Fermi surface and thus there is a minimum positive frequency required for absorption:

$$\omega\geq\frac{\hbar}{2m}(k_F^2-k_i^2)-(n+\tfrac{1}{2})\omega_c;$$
$$|k_F(n+1)|<|k_i|<|k_F(n)|, \quad (2.15)$$

and the corresponding q's satisfy ($k_i<0$) either

$$q\leq|k_i|-[k_F^2-(n+\tfrac{3}{2})k_c^2]^{1/2}, \quad (2.16)$$

or

$$q\geq|k_i|+[k_F^2-(n+\tfrac{3}{2})k_c^2]^{1/2}. \quad (2.17)$$

Owing to restriction (2.15), finite gaps will exist within the semiclassical absorption region (as shown in Figs. 1 and 2).

In order to study the absorption structure for different values of q in more detail, we consider transitions between adjacent levels of large and small n separately.

A. Inner Levels: $(n+\frac{1}{2})k_c^2 \ll k_F^2$

First consider transitions among low-lying levels. It is the small q transitions between these levels with the initial state close to the Fermi surface, that produce the

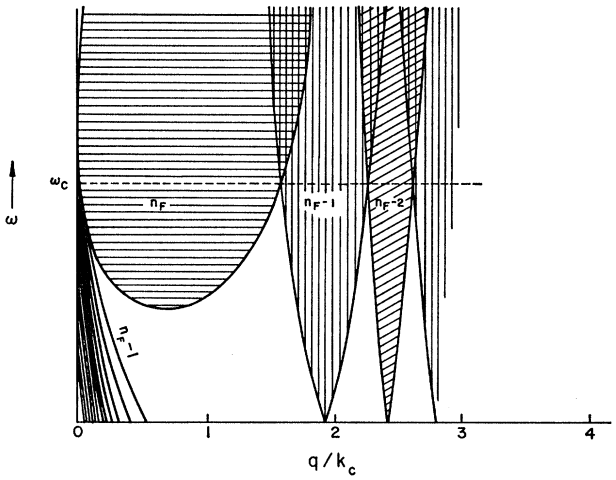

FIG. 2. Regions of the ω-q plane showing where the imaginary part of the dielectric constant is nonzero due to energy absorptions by electrons excited out of the outer filled Landau levels, $n\sim n_F$. In the case shown, the Fermi surface lies midway between the two Landau levels n_F and n_F+1 at $k_i=0$.

Doppler-shifted absorption edge.[9] For the case when $k_i=\pm k_F$ and $q\ll k_F$ in Eq. (2.9),

$$\omega=\omega_c\pm v_F q. \tag{2.18}$$

Transitions with electrons excited to states in the left half of the momentum space ($k_i<0\rightarrow k_i+q<0$) are governed by (2.15) and (2.16). Expanding to first order in $(k_c/k_F)^2$ we find the range of allowed q's for absorption to be $0\leq q<\omega_c/v_F\simeq 10^4$ cm^{-1}. These transitions cause the filamentary structure adjacent to the lower Kjeldaas edge ($0\leq\omega\leq\omega_c$) and which underly the giant quantum oscillations in helicon absorption[20,21] and attenuation of transverse sound waves.[23,24] The lower edge of the nth absorption filament comes from transitions initiating from the left intersection of the nth Landau cylinder with the Fermi surface. Upper and lower edges of successive filaments meet at $q=0$, representing vertical transitions to the left intersection of the $(n+1)$th cylinder. At nonzero q the slits between filaments increase in width and become broader than the absorbing regions. However, for small quantum numbers, the filaments are densely packed. This fine structure at $q\leq\omega_c/v_F$ is shown schematically in the lower left portion of Fig. 1. It is easily shown that the separation between filaments for $\omega=0$ is

$$\Delta q_{n,n+1}{}^{-}(0)\simeq\frac{1}{4}\left(\frac{k_c}{k_F}\right)^4 k_F\sim 10^{-9}k_F, \quad \text{small } n \tag{2.19}$$

while

$$q\sim\omega_c/v_F=\beta k_F\sim 10^{-4}k_F.$$

Now consider transitions between low-lying levels, but with the electron emergent into the right half of momentum space, $k_i+q>0$. Because of Pauli exclusion the final wave number must exceed $[k_F{}^2-(n+\frac{3}{2})k_c{}^2]^{1/2}$. Small momentum-transfer transitions initiating from positive k_i near this final wave number produce the upper Kjeldaas edge $\omega=\omega_c+v_F k_F$. But it is also possible for the electron to move from negative k_i all the way through the Fermi sphere and emerge near the right edge of the $(n+1)$st cylinder. Transitions from the left edge of the nth cylinder to this final state absorb almost $2k_F$ wave number, but zero frequency, while transitions from just beneath the left edge of the $(n+1)$st level to its extreme right edge absorb ω_c. These absorption bands coming from low-lying levels, with the electron traversing almost the entire Fermi diameter $2k_F=10^8$ cm^{-1} are shown on the right side of Fig. 1. The width of the gaps between the absorption regions can be calculated.

For $\omega=0$ we find

$$\Delta q_{n,n-1}{}^{+}(0)\simeq\left(\frac{k_c}{k_F}\right)^2 k_F\sim 10^{-4}k_F, \quad \text{small } n \tag{2.20}$$

while $q\sim 2k_F$. Though the gaps in this region are much smaller than q, they are as wide as the entire region below the Kjeldaas absorption edge up to $q=\omega_c/v_F$.

At frequencies greater than ω_c there are overlapping absorptions to which more than one level contributes. Here $\epsilon_2{}^{-}(\omega,q)$ is proportionately greater.

B. Upper Levels: $(n+\frac{1}{2})k_c{}^2\simeq k_F{}^2$

Absorption due to transitions from Landau levels near the maximum level intersecting the Fermi surface is sensitive to the value of the magnetic field, displaying the variations characteristic of the $1/H$ oscillations of all electronic properties as Landau levels move through the Fermi surface. These oscillations will be appreciated by consideration of two limits. First suppose the uppermost Landau level to coincide with the Fermi energy, so that there are no Pauli exclusion restrictions on transitions to this final state, and the filled initial states, which lie on the level $n=n_F-1$, have wave numbers in the range $|k_i(n_F-1)|\leq k_c$. Transitions from the left edge of the n_F-1 level to the point of tangency of the n_F level with the Fermi sphere absorb zero frequency and wave number $q=k_c\simeq 10^6$ cm^{-1}. Vertical transitions at $k_i=0$ absorb ω_c, and transitions from other initial states on the n_F-1 level fill the central parabolic absorption region. Transitions from (n_F-2) to (n_F-1) are divided by Pauli exclusion into two regions. As with absorptions from inner levels, filaments on the left meet at $q=0$, near where they are densely packed just as for small n. However for $q\sim k_c$ and $\omega=0$ the window widths between filaments is of the order of k_c which is comparable with q and much larger than the slits between small n filaments.

At the other limiting value of H, when the Fermi surface lies midway between two levels, the uppermost occupied level $n=n_F$ has all momentum states filled for wave numbers

$$|k_i(n_F)|\leq k_c/\sqrt{2}.$$

Absorptions due to transitions initiating on $n=n_F$ fill the central parabola of Fig. 2. It can be seen that the minimum frequency absorbed by such transitions, $\omega=\frac{1}{2}\omega_c$, occurs at $q=k_c/\sqrt{2}$. Other than this raising and shift of the highest-absorption band with a consequent central window width exceeding k_c, there are only quantitative differences between the two limiting situations. But in both situations the widest windows, near $q=k_c\simeq 10^6$ cm^{-1}, are 10^4 times wider than the filamentary slits near $q=\omega_c/v_F=10^4$ cm^{-1}.

Equation (2.24) shows the variation of magnetic field between the limiting situations to be

$$\Delta H=2eH^2/chk_F{}^2=4\times 10^{-9}H^2 \text{ G} \tag{2.21}$$

at metallic densities. In a field of 10^5 G an inhomogeneity of only 20 G will cause different regions to experience the dielectric constant corresponding to the two limiting situations. There will then be some absorption at all frequencies, making detection of the windows more difficult.

III. NONMAGNETIC METALS

We now study how the quantum structure of $\epsilon_2^-(\omega,q)$ modifies the propagation of electromagnetic waves through the metal. In this section we consider nonmagnetic metals, where $\mu(\omega,q)=1$.

At wave numbers far below the Kjeldaas edge, $q\ll\omega_c/v_F$ the quantum structure of $\epsilon_1^-(\omega,q)$ is not strongly felt. The semiclassical and quantum theories both give

$$\epsilon_1^{\pm}(\omega,q)=1-\omega_p^2/\omega(\omega\pm\omega_c). \tag{3.1}$$

Ignoring unity in (3.1) and substituting $\epsilon_1^-(\omega,q)$ into the general condition for propagation given by Maxwell's equations,

$$\omega^2=c^2q^2/[\mu(\omega,q)\epsilon(\omega,q)], \tag{3.2}$$

we obtain the dispersion relation for left-hand circularly polarized propagation

$$\omega=[c^2(\omega_c-\omega)/\omega_p^2]q^2. \tag{3.3}$$

Equation (3.3) has a low-frequency solution, the well-known helicon mode, with approximate quadratic dispersion law

$$\omega\simeq(c^2\omega_c/\omega_p^2)q^2;\quad q\ll\omega_c/v_F,\quad \omega\ll\omega_c. \tag{3.4}$$

At metallic densities and typical laboratory fields the frequency of this mode is much less than ω_c even up to the absorption edge, Eq. (2.18). As given by Eq. (3.4) the dispersion curve intersects the edge very close to $q=\omega_c/v_F$ with $\omega\simeq c^2\omega_c^3/(\omega_p^2v_F^2)$.

However, the actual dispersion relation departs considerably from Eq. (3.4) near and beyond the absorption edge. This departure is the result of two physical effects: The local dielectric constant of Eq. (3.1) is only appropriate in the small (ω,q) region; and within the absorption cone quantum structure in ϵ_2 enforces extreme oscillations in ϵ_1.

The semiclassical nonlocal dielectric function[8] is readily obtained by replacing sums by integrals in Eqs. (2.2) and (1.29) with the result

$$\epsilon_1^-=1+\frac{3}{4}\left(\frac{\omega_p}{\omega}\right)^2\left(\frac{1}{8z}\left\{[1-(u'-z)^2]^2\ln\left|\frac{1-u'+z}{1+u'-z}\right|\right.\right.$$
$$\left.-[1-(u'+z)^2]^2\ln\left|\frac{1-u'-z}{1+u'+z}\right|+\tfrac{1}{3}20z-12u'^2z-4z^3\right\} \tag{3.5a}$$
$$+u_c\left\{\frac{1}{2}[1-(u'-z)^2]\ln\left|\frac{1-u'+z}{1+u'-z}\right|+\tfrac{1}{2}[1-(u'+z)^2]\right.$$
$$\left.\left.\times\ln\left|\frac{1-u'-z}{1+u'+z}\right|-2u'\right\}-\frac{4}{3}\right),$$

where

$$u'\equiv u_c[(\omega/\omega_c)-1]. \tag{3.5b}$$

Neglecting terms of order β^2 and z^2, Eq. (2.3) for ϵ_2^- can be reduced to

$$\epsilon_2^-=\frac{3\pi}{4}\left(\frac{\omega_p}{\omega}\right)^2\frac{\omega_c}{qv_F}\left[\frac{\omega}{\omega_c}+\delta_1(\omega)-\delta_2(\omega)\right](1-x^2), \tag{3.6}$$

with $x=(\omega-\omega_c)/qv_F)$ and

$$\delta_1(\omega)=\tfrac{1}{2}-\frac{1}{2\beta}(1-x^2-z^2+2zx)\ \text{mod}1,$$

$$\delta_2(\omega)=\tfrac{1}{2}+\frac{1}{2\beta}(1-x^2-z^2-2zx)\ \text{mod}1.$$

In form (3.6) the quantum-mechanical ϵ_2^- has a more apparent relationship to the semiclassical form

$$\epsilon_2^{sc-}=\tfrac{3}{4}\pi\frac{\omega_p^2}{\omega qv_F}(1-x^2),\quad \epsilon_2>0 \tag{3.7}$$
$$=0,\quad \text{otherwise}.$$

However, Eq. (2.3) is both more accurate and more convenient for machine calculation.

In the semiclassical approximation $\epsilon_2^{sc-}(\omega,q)$ is nonzero everywhere within the cone.[8] Although there is no propagation in absorptive regions, it is nonetheless interesting to substitute (3.5) into (3.2) for comparison with both the local result (3.3) and with the quantum-mechanical solution soon to be studied. The conclusions of the nonlocal semiclassical analysis are depicted in Fig. 3. $\omega(q)$ follows the quadratic dependence of the local theory up to about $q=0.85\omega_c/v_F$. At higher wave numbers ω rises rapidly, joining onto a solution falling from ω_c at wave numbers slightly below ω_c/v_F. There is another such solution, also parallel to but infinitesimally beyond the absorption edge. It departs from the edge only at very small frequencies. $(\omega\sim10^{-4}\omega_c)$, extends to $q\sim2.9\times10^4$ cm^{-1}, and then doubles back onto a high-frequency mode descending from ω_c. At greater wave numbers there is no semiclassical solution.

The manifold distortions of the dispersion curve due to quantum structure are best understood by consideration of the Kramers-Kronig relation

$$\epsilon_1^{\pm}(\omega)=1+\frac{1}{\pi}\mathrm{P}\int_{-\infty}^{\infty}\frac{\epsilon_2^{\pm}(\omega')}{\omega'-\omega}d\omega', \tag{3.8}$$

with the P indicating a principal value integral. At a discontinuous rise in $\epsilon_2^-(\omega)$ as a function of frequency, $\epsilon_1^-(\omega)$ has a positive logarithmic singularity, and at a discontinuous decrease in $\epsilon_2^-(\omega)$ there is a negative logarithmic spike in $\epsilon_1^-(\omega)$. Thus the absorption fila-

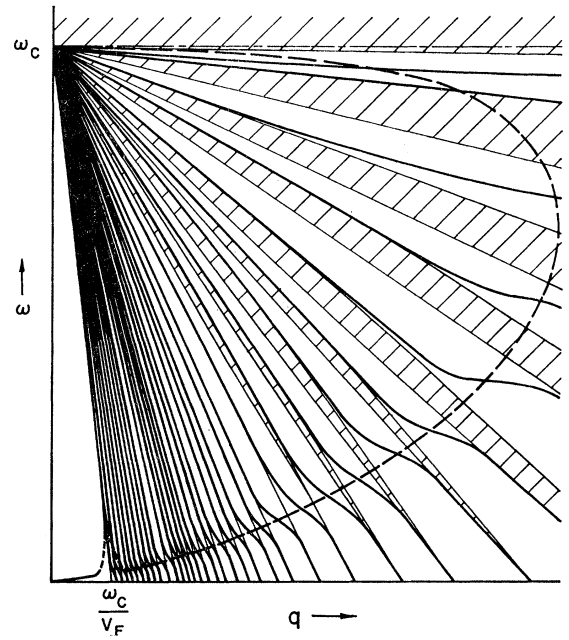

FIG. 3. Filamentary fine structure in $\epsilon_2^-(\omega,q)$ and electromagnetic modes within the slits in ϵ_2^-. Solutions of Maxwell's equations transfer from the upper edge of one absorption filament to the lower edge of the next, the transfer coming in the region of the semiclassical extension of the helicon mode. The semiclassical solution, shown as a dashed line, is not a single-valued function of q. It exists only for q below some limiting value ($q \simeq 2.9\times10^4$ cm^{-1} for the field and Fermi energy of Sec. II).

ments "repel" the mode and cause solutions of the dispersion relation (3.2) to lie between the edges of filaments rather than crossing them. Consider the region $q<\omega_c/v_F$. Here $\epsilon_2^-(\omega)$ is zero at frequencies below the absorption edge and is finite within each filament shown in Fig. 1. The behavior of $\epsilon_2^-(\omega)$ is illustrated in the upper portion of Fig. 4. Some general features of $\epsilon_2^-(\omega)$ not obvious in the Fig. 4, are that the width of the filaments increases with increasing ω, but the window widths are independent of ω and increase with q as q^2 up to ω_c.

At small q, and below the absorption edge, $\epsilon_1^-(\omega)$, as given by Eq. (3.1), varies as

$$\epsilon_1^-(\omega)\cong\omega_p^2/\omega_c\omega. \tag{3.9}$$

The dispersion relation is satisfied for that value of ω for which

$$\epsilon_1^-(\omega)=c^2q^2/\omega^2. \tag{3.10}$$

The right-hand side of Eq. (3.10) and $\epsilon_1^-(\omega)$ are plotted in the lower portion of Fig. 4. The low frequency crossing of the two curves is the ordinary helicon solution. For ω and q well below the absorption edge, the quantum and semiclassical solutions coincide. But as the mode approaches the edge, whereas the semiclassical solution rose toward ω_c along the edge, as shown by the dashed line in Fig. 3, the quantum-mechanical solution falls to zero frequency at $q=\omega_c/V_F$.

Now, at this same q, consider the behavior of $\epsilon_1^-(\omega)$ at much higher frequencies within the Doppler-shifted cone. The lower right side of Fig. 4 illustrates this behavior which is characteristic of regions in which the semiclassical $\epsilon_1^-(\omega,q)$ lies far above c^2q^2/ω^2. As ω increases toward the low-frequency edge of an absorption filament there is the logarithmic rise in $\epsilon_1^-(\omega)$. Within each filament as ω approaches the high-frequency edge $\epsilon_1^-(\omega)$ falls to negative infinity, and beyond the edge $\epsilon_1^-(\omega)$ rises again. Away from the discontinuities in $\epsilon_2^-(\omega,q)$ and over much of the frequency range one finds that $\epsilon_1^-(\omega,q)$ is a smooth and relatively slowly varying function which does not differ by very much from the semiclassical dielectric constant. Therefore, for fixed q, the only solutions to Eq. (3.10) come very close to the low-frequency edges of the nonabsorbing windows.

Next consider a wave number somewhat beyond ω_c/v_F. The nature of the solutions of Maxwell's equations differs in two regions of frequency, above and below a transition frequency which is in the neighborhood of the semiclassical helicon extension as indicated in Fig. 3. In the high-frequency region the situation

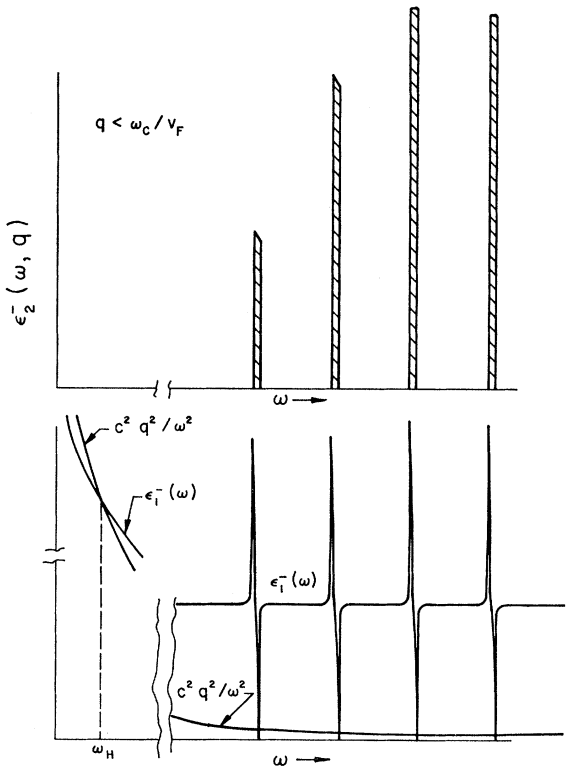

FIG. 4. Top: The imaginary part of the dielectric constant as a function of frequency for $q=0.9\omega_c/v_F$. In this case the first absorption onset comes at $\omega/\omega_c\simeq0.1$ and the succeeding onsets are spaced by $\Delta\omega/\omega_c\simeq0.9\beta$. Bottom: The corresponding real part of the dielectric constant for the same frequencies and c^2q^2/ω^2. Intersections of the two curves indicate a collective mode. ω_H is the helicon frequency, and in the case shown $\omega_H/\omega_c\sim10^{-5}$.

is as in Fig. 4 with a mode near the lower edge of each window. At frequencies below the helicon extension the average value of $\epsilon_1^-(\omega,q)$ is less than c^2q^2/ω^2 and it is the singular positive spike in $\epsilon_1^-(\omega,q)$ which enforces solutions of Eq. (3.2) very close to the lower edges of absorption bands. The width of the transition region, where the modes change from the low to the high side of a transmission window, increases with wave number and moves to higher frequencies as q approaches $\sim 10\omega_c/v_F$.

Beyond that region the modes all lie near the high-frequency edges of the windows. At $q=10^5$ cm^{-1}, $\Delta n=1$ transitions between only about ten of the highest filled Landau levels contribute to the dielectric constant. Absorption bands, caused by transitions in which the electron both initiates and emerges in the left half of momentum space, are broader here. There is also a continuous broad region of nonzero $\epsilon_2^-(\omega,q)$ extending well below ω_c due to the top filled level. In Fig. 5 we show $\epsilon_2^-(\omega,q)$ as a function of ω/ω_c at $q=1.1\times10^5$ cm^{-1}. For $\omega>0.7\omega_c$, the imaginary part of the dielectric constant is large and decreases slowly until additional levels can contribute to the absorption near ω_c. Figure 5 also shows $\epsilon_1^-(\omega,q)$ as a heavy solid line and c^2q^2/ω^2 as a dashed line. Crossing of these two lines in a region of vanishing $\epsilon_2^-(\omega,q)$ indicates the solution of the dispersion relation (3.9) which here occurs on the lower edges of absorption bands.

Lifetime effects due to electron-electron interactions, electron-phonon interactions, or impurity scattering could smooth the absorption structure we have described and broaden or completely damp out the collective modes. We have not carried out a detailed analysis of these collision effects; however, the observation of oscillations in magnetoacoustic absorption leads one to expect that structure in electromagnetic absorption such as we have described should also persist and be observable.

Recently Quinn[20] and Miller[21] independently proposed that there should be giant oscillations in the attenuation of the helicon mode near the absorption edge. In terms of the present analysis, the propagating modes beyond the Kjeldaas edge have been found to transfer from one to the other side of their transmission region in the neighborhood of the semiclassical helicon extension. Thus we are in accord with Quinn's and Miller's conclusions provided we understand the quantum extension of the helicon to consist of a window mode in its region of transfer between edges. The helicon then experiences giant oscillations in attenuation as one follows the semiclassical dispersion curve through successive filaments and windows. The present detailed analysis also shows however, that it will be very difficult to observe this structure. The usual surface impedance measurements are unsuited to this purpose. In a typical study of the helicon mode near the absorption edge, microwave radiation of fixed

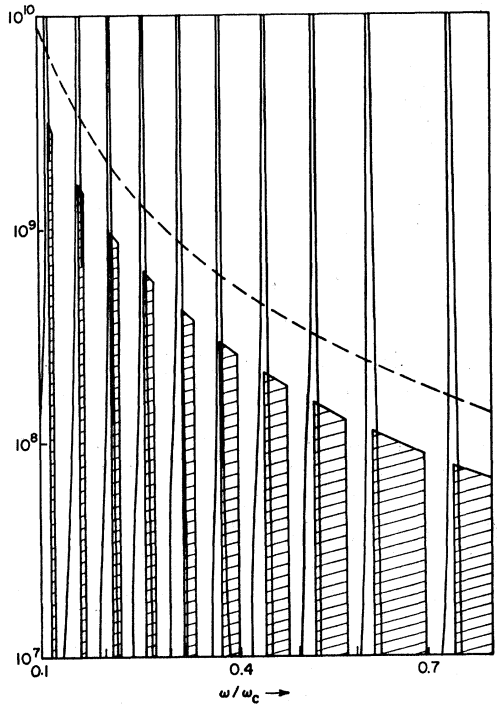

FIG. 5. The dielectric constant as a function of frequency for $q=1.1\times10^5$ cm^{-1}. At this value of q only about ten of the highest filled Landau levels contribute to $\epsilon_2^-(\omega,q)$. The frequency regions where these contribute are shaded in the figure. The real part of $\epsilon^-(\omega,q)$, indicated by solid lines in the figure, exhibits logarithmic singularities at discontinuities in $\epsilon_2^-(\omega,q)$. Propagating solutions to Maxwell's equations occur at frequencies for which $\epsilon_2^-(\omega,q)$ is zero and $\epsilon_1^-(\omega,q)$ crosses the dashed line representing c^2q^2/v^2. For wave numbers in the range $2.9\times10^4<q<k_c\simeq7.8\times10^5$ cm^{-1}, these modes all occur near the upper edges of the transmission windows.

frequency is incident on the sample and the magnetic field is varied until there is a sudden change in the surface impedance. In terms of Fig. 3 notice that the effect of changing the field is equivalent to changing the scale since ω_c is proportional to H. Thus increasing the field is equivalent to moving to a relatively lower applied frequency ω on Fig. 3. There will be no helicon mode at a given frequency unless the field is increased to a point where the helicon emerges from the absorption edge. At this point one can expect the surface impedance to change markedly. For weaker fields (or higher frequencies), however, the surface impedance depends on the distribution of absorption strength over a wide range of wave numbers. The relation between surface impedance $Z(\omega)$ and volume energy absorption depends on the boundary conditions at the metallic surface. Pippard[25] reviews the relationship in two limiting cases. For specular reflection at the surface,

$$Z(\omega)=8i\omega\int_0^\infty \frac{dq}{q^2-(\omega^2/c^2)\epsilon(q,\omega)} \quad \text{(specular)}, \quad (3.11)$$

[25] A. B. Pippard, Rept. Progr. Phys. **23**, 176 (1960).

while for a diffuse surface condition,

$$Z(\omega)=\frac{4\pi^2 i\omega}{\int_0^\infty \ln[1-(\omega^2/q^2c^2)\epsilon(q,\omega)]dq} \text{ (diffuse)}. \quad (3.12)$$

In general one would expect $Z(\omega)$ to depend on an integral of the form

$$I(\omega)=\int_0^\infty f(q,\omega)dq,$$

where $f(q,\omega)$ is a function of $q^2-(\omega^2/c^2)\epsilon(q,\omega)$. A plot of $f(q,\omega)$ appropriate to the real part of Eq. (3.11) (surface resistance) is shown in Fig. 6 for three typical frequencies: (i) where the helicon is a definite independent mode and the first few windows near the Kjeldaas edge; (ii) near the helicon absorption edge; and (iii) a frequency above the absorption edge. When the helicon exists it almost completely dominates the surface impedance. Closer to the absorption edge more energy goes into the single particle excitations and edge modes, but the helicon can be expected to continue to dominate the surface impedance up to the point where its group velocity vanishes. Beyond the cutoff, energy goes into many close-lying modes and no single mode dominates the absorption. As the field is now varied the absorption pattern changes continuously. Even if one propagation mode moves across the window there will be no marked variation in the surface impedance since any one of these modes contains little of the total available "oscillator strength."

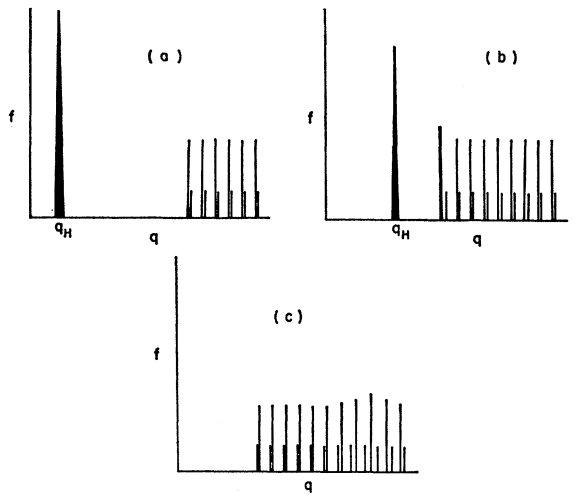

FIG. 6. Schematic plot of the integrand F of Eq. (3.8) for three typical frequencies: (a) where the helicon is a definite independent mode; (b) a higher frequency, closer to the helicon absorption edge; and (c) a frequency above the absorption edge. Below the cutoff the helicon almost completely dominates the surface impedance. The lowest peaks indicated in each of these figures are the absorption filaments which are much narrower than the windows in the cutoff frequency region near the Kjeldaas edge.

How then can one observe this structure? In magnetoacoustic absorption the situation differs from that in the pure helicon case since the phonons are characterized by their own dispersion. For each ω, the phonons have a definite q, and the energy exchange between the phonon and electron systems can be said to occur at particular points on the ω, q plane. As either ω or the magnetic field is varied the absorptions follow a trajectory which crosses filaments and exhibits the full variation in attenuation rather than an average attenuation. In order to observe oscillations in helicon absorption, it will also be necessary to fix externally any two of the three variables ω, q, H and by varying the remaining variable sweep either vertically or horizontally through Fig. 3. Experiments which can fix two variables in this way are possible. One potentially useful method appears to be Raman scattering with lasers providing the high intensity, very coherent beams necessary to resolve such detailed effects. The angle between the initial and detected signal determines the momentum transfer q to the modes being excited in the material. The energy transfer can be determined as the beat frequency between the incident and scattered beams. Near the Kjeldaas edge the windows and filament are very narrow and there remains the difficult problem of resolving extremely small angles (on the order of microradians at about 10 mrad). Further into the absorption cone, however, the filaments and windows become considerably wider so that resolution should not be as difficult.

We now turn to consideration of ferromagnetic metals and the possibility of propagation when the permeability can vary over a wide range.

IV. HELICON PROPAGATION IN FERROMAGNETS

In a ferromagnet the dispersion relation (1.3) can be strongly altered by the permeability $\mu(\omega,q)$. As in Ref. 12, we find $\mu(\omega,q)$ from the Landau-Lifshitz equation,[26]

$$\frac{d\mathbf{M}}{dt}=\gamma(\mathbf{M}\times\mathbf{H})+\frac{\alpha}{M_s}\mathbf{M}\times\nabla^2\mathbf{M}. \quad (4.1)$$

Here $\mathbf{M}$ is the total magnetization, including its precessing part $\mathbf{M}_\phi$ and its saturation component $\mathbf{M}_s$. The magnetic field $\mathbf{H}$ also consists of a precessing term $\mathbf{H}_\phi$ and a dc term $\mathbf{H}_m$:

$$\mathbf{H}_m=\mathbf{H}_0+\mathbf{H}_{\text{demag}}+\mathbf{H}_{\text{anis}}. \quad (4.2)$$

$\mathbf{H}_m$ is the effective field acting on the system, corrected for demagnetization and magnetic anisotropy. The coefficient $\gamma=ge/2mc$ and α is the exchange stiffness in the spin-wave dispersion relation

$$\omega_m=\gamma H_m+\alpha q^2. \quad (4.3)$$

[26] L. Landau and E. Lifshitz, Physik Z. Sowjetunion 8, 153 (1935).

Solution of (4.1) leads to the conventional permeability

$$\mu^-(\omega,q)=1+[4\pi\gamma M_s/(\omega_m-\omega)]. \quad (4.4)$$

This permeability is real because we have ignored loss terms in the Landau-Lifshitz equation. Inclusion of such terms, and hence of a $\mu_2^-(\omega,q)$ in (4.4), would alter both the real and imaginary parts of the product $\mu\epsilon$. With the permeability of Eq. (4.4) we shall again find that in regions in which $\epsilon_2^-(\omega,q)=0$ there are propagating solutions of Maxwell's equations, but now they are coupled helicon-magnon modes and are physically quite different and more complicated than the modes discussed in the previous section.

In the numerical calculation of the dielectric function by Eqs. (2.2) and (2.3) we chose $\omega_c=3.5\times10^{11}$ sec^{-1}, implying a magnetic induction $B=2\times10^4$ G. To conform to this value we can consider the application of an appropriate external field in

$$B=H_0+4\pi M_s. \quad (4.5)$$

Thus for nickel, in which $4\pi M\cong6000$ Oe, we take $H=14\,000$ Oe. We shall take an anisotropy field of $H_{\text{anis}}\cong1000$ Oe, and an exchange stiffness $\alpha=0.1$ cm^2 sec^{-1}. These values are somewhat arbitrary. The anisotropy field is not operative in the Lorentz field B of Eq. (4.5), which is the field acting on a moving charge, but it is included in the field H of Eq. (4.2), which is the field acting on a spin. Because of anisotropy the zero frequency and zero wave number permeability is not infinite even in zero external field. In the case of nickel $\mu_0(0,0)=7$. Consider the permeability of Eq. (4.4) as a function of ω/ω_c. At zero frequency, it is finite and positive, rising to ∞ as $\omega\to\omega_m^-$, reversing to $-\infty$ at ω_m^+, and rising to unity as $\omega\to+\infty$.

The behavior of $\mu^-(\omega,q)$ has important effects on the solution of Eq. (3.2):

$$\mu(\omega,q)\epsilon(\omega,q)=c^2q^2/\omega^2. \quad (4.6)$$

First of all, since the right-hand side of Eq. (4.6) is positive, solutions exist only if $\epsilon_1^-(\omega,q)$ and $\mu^-(\omega,q)$ have the same sign. Secondly, the large permeability near ω_m has an effect similar to that of the large ϵ_1 near absorption edges, as illustrated in Figs. 3–5. That is, as a coupled mode approaches ω_m it "sticks," running parallel to and eventually merging into a pure magnon branch at large q.

Stern and Callen[12] employed Eqs. (4.4) and (3.1) in Maxwell's equations to arrive at the solutions

$$\omega=\tfrac{1}{2}(\omega_h+\omega_m)+\frac{2\pi\gamma M_s}{1+K^2}\pm\left[\left(\tfrac{1}{2}(\omega_h+\omega_m)+\frac{2\pi\gamma M_s}{1+K^2}\right)^2-\omega_m\omega_h\right]^{1/2}, \quad (4.7)$$

where

$$\omega_h\equiv\omega_c/[1+(1/K)^2] \quad (4.8)$$

is the frequency of the uncoupled helicon and

$$K\equiv qc/\omega_p \quad (4.9)$$

is the reduced wave number, in terms of the Pippard wave number, or skin depth. At the long- and short-wavelength limits, the two solutions of Eq. (4.7) reduce to

$$\omega=\mu(0,q)\omega_m,\ \omega_h/\mu(0,q),\quad K\ll1 \quad (4.10)$$

$$\omega=\omega_c,\ \omega_m,\quad K\gg1. \quad (4.11)$$

In the long-wavelength limit the spin-wave mode is shifted up by $4\pi\gamma M_s$ and the curvature of the electromagnetic mode reduced by $\mu(0,q)$. The shift in the spin-wave spectrum at $q=0$ is not due to demagnetization effects in the infinite medium considered here, nor even due to high-conductivity helicon effects, but only to displacement currents.[27,28] (It should be noted that this solution is for an infinite medium. For finite samples the demagnetization field H_{demag} of Eq. (4.2) can shift the spin-wave mode greatly, moving it all the way back down to zero frequency for normal incidence on an infinite plane, for example.) However, the dispersion relation (4.7) at nonzero wave number is peculiarly a high-conductivity effect. The predicted electromagnetic mode at small q of Eq. (4.10) has now been confirmed in quantitative detail in nickel.[29]

Because Stern and Callen[12] employ the semiclassical dielectric function of Eq. (3.1), their spectrum (4.7) is applicable in the long-wavelength range of Eq. (4.10), but is incorrect inside the Doppler-shifted absorption cone, where they predict absorption of coupled modes. We wish now to consider the modifications of this spectrum caused by the nonlocal semiclassical and quantum-mechanical dielectric functions.

First let us recall the behavior of the nonlocal semiclassical solution of Maxwell's equations in a nonmagnetic metal. As shown in Fig. 3 the solution is a complicated function of q, extending to a $q\sim2.9\times10^{-4}$ cm^{-1}, where $\omega/\omega_c\sim0.5$, and returning to ω_c at $q=0$. For purposes of comparison this curve is repeated in Fig. 7 on a logarithmic scale. The effect of the permeability at low frequencies is to depress the dispersion curve by the factor μ, as in Eq. (4.10). As ω increases with increasing q, the permeability becomes larger and the deviation from the nonmagnetic solution becomes greater. This behavior is illustrated as the coupled-magnetic mode in Fig. 7. Now the curve is single valued because $\mu(\omega,q)$ is negative for $\omega>\omega_m$, while $\epsilon_1^-(\omega,q)$ remains positive in that region. At large q the magnetic solution asymptotically approaches the bare magnon, shown as a dashed line in Fig. 7. The frequency of this undressed mode is given by Eq. (4.3). Because of the large permeability the coupled mode thus extends out

[27] C. Kittel, *Quantum Theory of Solids* (John Wiley & Sons, Inc., New York, 1963), p. 47.
[28] P. Pincus, J. Appl. Phys. **33**, 553 (1963).
[29] C. C. Grimes, Bull. Am. Phys. Soc. **10**, 471 (1965).

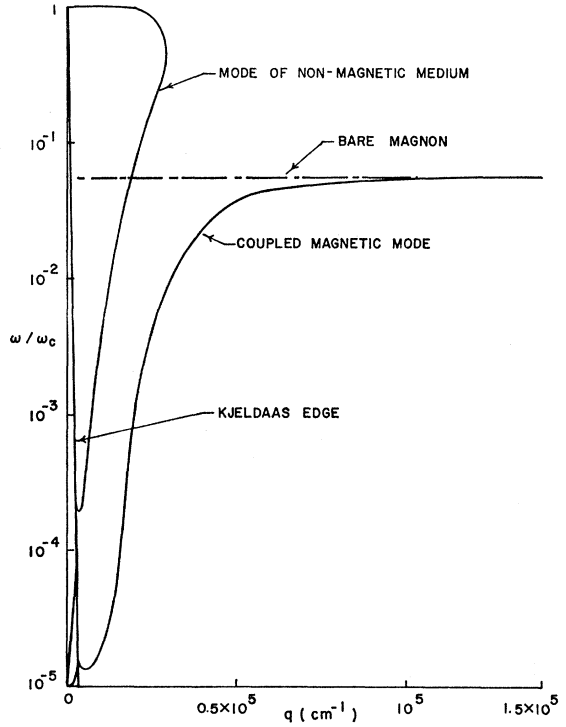

FIG. 7. Semiclassical dispersion curve of a ferromagnetic metal. At large wave numbers, $\omega(q)$ asymptotically approaches the bare spin-wave frequency, shown as a dashed line. For comparison the semiclassical dispersion curve of a nonmagnetic metal is also shown.

to large q, ultimately reverting to a pure spin wave [the ω_m limit of Eq. (4.11)].

Now let us consider the effect of magnetic coupling on the quantized medium. For $q<k_c$ the results are qualitatively similar to the nonmagnetic case and imply propagating modes such as those indicated in Fig. 3. Now, however, the large permeability shifts the frequencies to lower values. Again modes shift from the upper edge of one absorption filament to the lower edge of the next, and just as in the nonmagnetic case, the transfer occurs near the semiclassical dispersion curve of Fig. 7.

For $q\gtrsim k_c$, the coupled magnon-helicon mode traverses the large windows in $\epsilon_2^-(\omega,q)$. The behavior is illustrated in Fig. 8. Modes run up a window edge, across near ω_m, and down the next edge. Within the windows are some regions of negative $\epsilon_1^-(\omega,q)$, and here the mode actually shifts slightly through ω_m to a negative permeability region. At $q>1.8k_c$, the spin-wave frequency ω_m rises above ω_c, and hence $\mu>0$ within all further windows. However $\epsilon_1^-(\omega,q)$ is positive hereafter only along window edges, so for $q>2k_c$ there are only edge modes, until the pure uncoupled spin wave emerges from the absorption region at very high frequency and at $q>2k_F\simeq 10^8$ cm^{-1}.

As in the nonferromagnetic case, there are lifetime

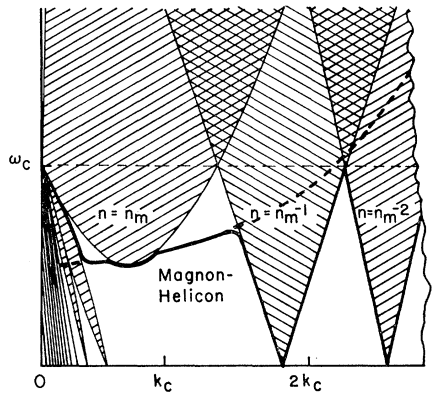

FIG. 8. Window region of the ω-q plane. The solid line shows the dispersion curve of the coupled helicon-magnon mode in a ferromagnetic metal. For q near k_c the dashed line shows the semiclassical dispersion curve which asymptotically approaches that of an uncoupled spin wave. For $q<1.8k_c$ the spin-wave frequency is smaller than ω_c and the mode passes through large nonabsorbing windows. For larger q the solutions follow the window edges until for $q\simeq 10^8$ cm^{-1} the spin wave reemerges from the electronic absorption cone.

effects which will damp the modes. Now a τ_m must also be introduced to describe magnetic damping, which was neglected through use of Eq. (4.4) and the omission of loss terms in the Landau-Lifshitz equations. However, if electronic effects are the dominant loss mechanism it should be possible to observe the coupled helicon-magnon mode in the large window regions with $q\sim k_c$.

Nickel is a suitable material in which to observe helicon-magnon interaction both because it can be purified sufficiently and because it is uncompensated. Saturation of the magnetoresistance, and Hall-voltage measurements indicate that nickel behaves as if it had one free electron per atom.[30] On the other hand, iron may be compensated. Spector and Casselman[31] have given the local theory of the interaction of Alfven waves and spin waves appropriate to a compensated ferromagnet below the Kjeldaas edge when the $\omega_c\tau_i$ condition is satisfied by both electrons and holes. The quantum theory of the dielectric tensor within the absorption cone of a compensated metal and of Alfven-magnon coupling have not been given.

ACKNOWLEDGMENTS

We acknowledge helpful discussions with Dr. Edward A. Stern. One of us (A.J.G.) would like to thank the Aspen Institute of Humanistic Studies for hospitality during an early stage of this investigation. Computer time for this project was supported in part by the National Aeronautics and Space Administration under Grant No. NsG 398, to the Computer Science Center of the University of Maryland.

[30] E. Fawcett and W. A. Reed, Phys. Rev. **131**, 2463 (1963).
[31] H. N. Spector and T. N. Casselman, Phys. Rev. **139**, A1594 (1965).